Exciton annihilation as bimolecular loss in organic solar cells

Lior Tzabari, Victoria Zayats, and Nir Tessler

Citation: Journal of Applied Physics **114**, 154514 (2013); doi: 10.1063/1.4825048
View online: http://dx.doi.org/10.1063/1.4825048
View Table of Contents: http://scitation.aip.org/content/aip/journal/jap/114/15?ver=pdfcov
Published by the AIP Publishing

Exciton annihilation as bimolecular loss in organic solar cells

Lior Tzabari, Victoria Zayats, and Nir Tessler[a)]
Microelectronic & Nanoelectronic Centers, Electrical Engineering Department, Technion Israel Institute of Technology, Haifa 32000, Israel

(Received 30 May 2013; accepted 27 September 2013; published online 18 October 2013)

The dependence of the internal quantum efficiency of P3HT:PCBM (Poly(3-hexylthiophene-2,5-diyl) :[6,6]-Phenyl C61 butyric acid methyl ester) solar cell on light intensity was measured over four orders of magnitude and for devices annealed for 4 and 10 min. We find that both trap assisted (Shockley-Read-Hall type) and bimolecular losses coexist, the relative magnitude of which is dependent on both the light intensity and the processing conditions. We suggest that the use of Langevin type charge recombination in conjunction with trap assisted recombination is not the best choice and show that the well-known exciton annihilation by charge polaron may better account for the bimolecular losses. © *2013 AIP Publishing LLC*. [http://dx.doi.org/10.1063/1.4825048]

Organic Photovoltaic cells (OPVs) are the subject of extensive research and development as they emerge to become a low cost, easy to produce, flexible, and efficient solution for converting the solar energy into electrical power.[1–4] One of the most studied structures of the organic solar cells is the Bulk-Heterojunction (BHJ) configuration.[5,6] To design more efficient OPVs there is a need to identify the physical processes that govern the operation of these devices and understand how to manipulate and control them. By having this ability, one can decide which directions to follow and where to aim in order to achieve better devices. For now, the main obstacle is the ambiguity found in various reports. Using the same set of measurements, different conclusions are drawn pointing to different physical processes as the limiting ones.

To be able to study the generation and recombination and more importantly separate the effects, we developed a technique that is based on sweeping the excitation intensity from ultralow intensity (10^{-3} sun) and up to high intensity (few sun).[7,8] The ultralow intensity regime is often considered irrelevant to solar cells since at such low intensity the "problems" associated with charge recombination within the device and/or bad contacts (i.e., recombination at the contacts) do not show up. This is exactly why we can use the ultralow intensity to directly measure the charge generation efficiency. As we ramp up the intensity the "problems" start to kick in one by one and from their evolution as a function of light intensity we can deduce the nature of the "problem" or the mechanism driving the loss of efficiency. Here, we use this technique to analyze the quantum efficiency of BHJ Poly(3-hexylthiophene-2,5-diyl) (P3HT):[6,6]-Phenyl C61 butyric acid methyl ester (PCBM) devices subjected to different annealing times. Results of our modeling show that in order to account for the full intensity range and different annealing time, we have to introduce a new recombination mechanism. This "new" mechanism is not charge-recombination but rather exciton recombination or annihilation by the generated charges. While such a mechanism is well known[9] and has been identified in P3HT:PCBM films using time-resolved microwave conductivity[10,11] and picosecond time resolved optical spectroscopy,[12,13] it is not being used to describe working devices. In a previous publication[8] we reported somewhat similar measurements; however, the excitation spot in those measurements was broad, thus introducing spurious edge effects which obscured the presence of bimolecular loss.

OPVs were fabricated using the following procedure: Cleaned patterned ITO substrates were put in UV-ozone for 15 min and then spin coated with PEDOT:PSS (Poly(3,4-ethylenedioxythiophene)-poly(styrenesulfonate)) (Baytron AL4083) creating a layer of 40 nm. The PEDOT layer was dried in air for 15 min using 110 °C hot plate. A solution of P3HT(Reike):PCBM (Nano-C)(1:1 ratio, 20 mg/ml) in 1,2-Dichlorobenzene (DCB), dissolved by heating and stirring overnight, was then spin coated on top of the PEDOT creating a 190 nm thick active layer. Eventually, top electrode of 10 nm Ca/120 nm Al/50 nm Au was evaporated at 10^{-6} mbar, followed by annealing of the devices at 135 °C for 4 min using a vacuum oven. This procedure resulted in 1.5%–2% power conversion efficiency (PCE) OPVs. Typical I-V and spectrally resolved external quantum efficiency are shown in Figure 1.

To gain better insight we also tested devices that were annealed for 10 min. The excitation was achieved using white Light emitting diodes (LEDs), and the intensity was scanned by both varying the LED current and using Neutral Density filters. Care was taken to ensure that all the light falls within the pixel so as to avoid any edge effects.

Figure 2 shows the measured quantum efficiency ($V = V_{SC}$) normalized to its value at the low intensity end. To bring out even a slight efficiency loss we zoom on the results by bringing the minimum of the Y axis to 0.5. We found that cells of different PCE would have similar normalized curves with better devices showing less than the 30% drop at 1 sun and worse showing higher drop. Namely, the loss strength may vary, but the loss mechanisms stay the same (we do not attempt here to study the effect of different processing conditions and/or additives). The results clearly show that at about 0.1 mW/cm^2 efficiency loss starts to be noticeable, and the different shape between the two annealing times suggest that there is more than one loss mechanism

[a)]Email: nir@ee.technion.ac.il. URL: www.ee.technion.ac.il/orgelect.

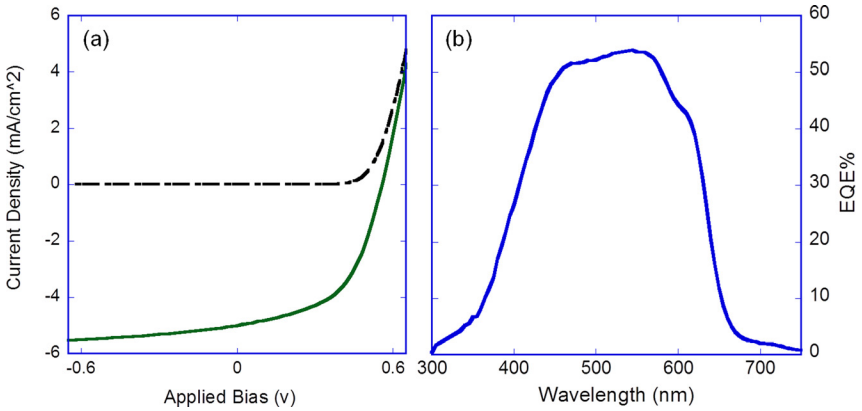

FIG. 1. (a) Current voltage characteristics in the dark (full line) and under 1 sun (dashed line). The cell exhibits $V_{OC} = 0.55$ V; $J_{SC} = 5$ mA/cm^2; FF = 0.5; PCE = 1.5%. (b) Spectrally resolved external quantum efficiency measured with an average light intensity of 1.5 μW/cm^2 and lockin frequency of 10 Hz.

at play. Few models to predict the QE of an OPV were presented in the past, taking into account or neglecting several physical processes.[7,14–16] In this paper we will base our analysis on the simple model presented by Rappaport *et al.*[7] which showed using two consecutive papers[7,17] that as long as the electron and hole mobilities are of the same order of magnitude capturing the physical essence does not require detailed drift-diffusion analysis.[17]

The Rappaport model use two assumptions: (1) Under sufficiently low excitation power the cell's efficiency is constant and is directly related to the generation efficiency in the absence of non-geminate recombination. (2) The loss mechanisms associated with non-geminate recombination take place at higher excitation intensity. As Figure 2 shows, we may retain the assumption that at sufficiently low light intensity the cell's efficiency is constant, and hence we also represent the photocurrent under low light intensity as

$$J_{PC} = A(V) \cdot P,$$

where A is a bias (electric field) dependent constant which represent the efficiency of the generation and dissociation processes, V is the internal voltage of the cell ($V = V_{bi} - V_{appl}$), V_{appl} is either the applied or photo-generated voltage, V_{bi} is the internal voltage at short-circuit, and P is the incident optical power density. This is also justified by the fact that at 10^{-4} sun the average distance between generated carriers is larger than the device dimensions such that non-geminate recombination is not likely to take place.

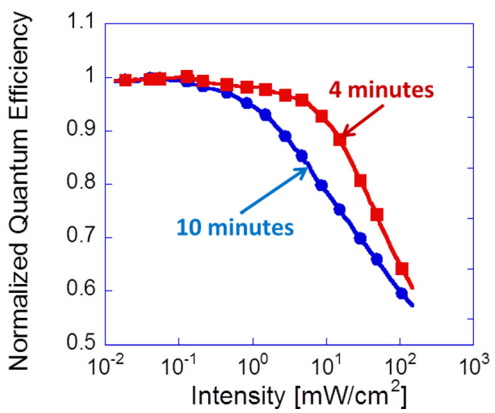

FIG. 2. Measured normalized quantum efficiency for devices annealed for 4 min (square symbols) and 10 min (round symbols).

As the excitation power increases, few loss mechanisms may set in. These loss mechanisms decrease the extracted photocurrent and thus a decrease in the cell's efficiency. For this region, the extracted photocurrent can be expressed as

$$J_{PC} = A(V) \cdot P - J_{loss}, \tag{1}$$

where J_{loss} stands for current loss (recombination current) that sets in at higher excitation intensity, and $A(V) \cdot P$ is the "ideal" photocurrent that could be extracted from the cell if there were no such losses. If we restrict our analysis to $V \gg kT$ (i.e., not too close to open circuit voltage where $V = V_{bi} - V_{appl} = 0$) than we can neglect diffusion currents and write[7]

$$J_{PC} = q\mu_e \frac{V}{d} n_e = q\mu_h \frac{V}{d} n_h. \tag{2}$$

The equality between the electron and hole currents exiting the device is valid mainly under steady state where any charging has stopped. Since we are interested here in steady state properties, we do not go into the details of when it may break.

Equation (2) may cause the impression that the photocurrent is always bias dependent but one should note that in the absence of loss mechanism and assuming a bias independent generation rate the current is fixed at $J_{PC} = A \cdot P$ and the quantity that changes with voltage is the charge density according to $n_h \approx J_{PC} \frac{d}{\mu V q}$ (also valid only for $V \gg kT$).

To analyze the results presented in Figure 2 we need to go beyond the Rappaport model, and hence instead of using the parameter A for the charge generation efficiency we describe the charge generation through a set of rate equations. To do so we follow the process where photons are absorbed at a rate G thus generating excitons (n_{ex}). These excitons may either recombine at a rate K_r, dissociate to charges at a rate K_s, or be annihilated by charge polarons (n_h). In Eq. (3) we sum the recombination rate and the dissociation rate as K_d, and $K_{ep}n_h$ is the exciton annihilation rate. The charges are directly generated from excitons, and the fraction α in Eq. (3) ensures that we count only the excitons that dissociate into charges ($\alpha = K_S/[K_S + K_r]$). Equation (3) also shows that the generate charges may either exit the device to form the photocurrent ($\mu n_h V/d$) or be lost through recombination at a rate R_{Loss}

$$\begin{cases} \frac{d}{dt} n_{ex} = G - n_{ex} \cdot K_d - n_{ex} \cdot K_{ep} \cdot n_h \\ \frac{d}{dt} n_h = \alpha \cdot n_{ex} \cdot K_d - \mu \frac{V}{d^2} n_h - R_{Loss}. \end{cases} \tag{3}$$

Based on Eq. (3) and assuming steady state we can write the generation current as

$$J_G = Gqd = (n_{ex} \cdot K_d + n_{ex} \cdot K_{ep} \cdot n_h)qd. \tag{4}$$

With these definitions the quantum efficiency can be written as

$$QE = \frac{J_{PC}}{J_G} \equiv \frac{J_{PC}}{J_{PC} + J_{loss}}. \tag{5}$$

As Eq. (5) shows, any difference between the generation current and the measured current would constitute losses which are collectively termed as J_{loss}. In Eq. (6) we collate all the loss mechanisms considered here. First, the charge recombination loss (R_{loss}) is potentially composed of Langevin recombination rate. Second, the Shockley-Read-Hall (SRH) trap assisted recombination. The third term is the well known exciton annihilation process via exciton-polaron collision.[9] This mechanism was recently invoked to account for intensity dependent photoluminescence measurements in P3HT:PCBM blends[10]

$$\begin{cases} R_{Lang} = K_{Lang} \cdot (n_e n_h - n_i^2); & J_{Lang} = R_{Lang} qd \\ R_{SRH} = \dfrac{C_n N_t [n_h n_e - n_i^2]}{(n_e + n_h) + 2n_i \cdot \cosh\left(\dfrac{\Delta E_t}{kT}\right)}; & J_{SRH} = R_{SRH} qd \\ R_{ep} = n_{ex} \cdot K_{ep} \cdot n_h; & J_{ep} = R_{ep} qd. \end{cases} \tag{6}$$

In Langevin theory $K_{Lang} = \frac{q}{\varepsilon}(\mu_e + \mu_p)$ however in the context of bulk heterojunction it is common the use K_{Lang} as a fitting parameter so as to account for the reduced charge recombination in such blends. In the SRH theory C_n is the charge capture coefficient, N_t is the trap density, and ΔE_t is the trap position relative to the middle of the gap. Considering the above loss mechanisms, since they are negligible at very low light intensity one can show that at the low light intensity $QE = \alpha$ (the free-charge generation efficiency).

In Figure 3 we use the above equations to demonstrate the usefulness of measuring the internal quantum efficiency starting from ultralow light intensity. The dashed blue line shows the intensity dependence of the quantum efficiency as calculated using Eqs. (4)–(6) and assuming that only the SRH loss mechanism is active ($K_{Lang} = K_{ep} = 0$). The blue circles show the power law, with respect to charge density, that is associated with the SRH recombination. We note that

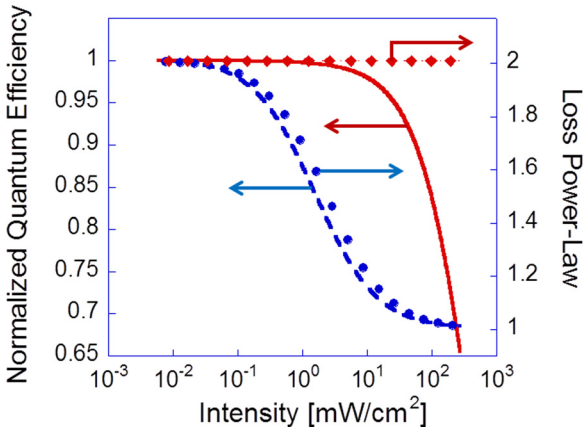

FIG. 3. Calculated normalized quantum efficiency (left axis) and the power low of the loss mechanism with respect to the charge density (right axis) as a function of light intensity ($V = V_{SC}$). The efficiency shown by the dashed blue line is for the loss mechanism being SRH, and the full red line is for the loss mechanism being either Langevin or exciton-polaron. The blue circles describe the SRH power law, and the red diamonds show the bimolecular nature of both Langevin and exciton-polaron loss mechanisms.

the SRH rate starts as a bimolecular process, and once the traps are filled it becomes a monomolecular process. As was discussed in Ref. 8 the position at which the efficiency starts to drop is mainly determined by ΔE_t and the level to which it drops is mainly determined by N_t. The full line shows the intensity dependence of the quantum efficiency assuming the only loss mechanism being either only Langevin or only exciton annihilation by polarons (holes in the P3HT). We note that both show the same signature associated with bimolecular process, and with the parameters chosen for K_{Lang} and K_{ep} the effect is identical.

Figure 3 shows that by scanning the excitation intensity starting at very low intensity one can introduce the loss mechanisms one after the other and thus better separate between them. It also shows that the exciton annihilation by charge polarons has a signature that is very similar to that of a bimolecular charge recombination (see also Eq. (7)). For completeness we state that if one would calculate the power law with respect to the excitation intensity, then the power laws would be smaller at the high intensity range where the charge density becomes sub linear with respect to the excitation intensity.

To complete the picture and provide some intuitive understanding of the results we use the above equations to approximate the loss mechanisms under different physical circumstances (see Eq. (7))

$$\begin{cases} R_{SRH} \approx \begin{cases} \dfrac{C_n N_t}{2n_i \cdot \cosh\left(\dfrac{\Delta E_t}{kT}\right)} [n_h n_e - n_i^2]; & (n_e + n_h) \ll 2n_i \cdot \cosh\left(\dfrac{\Delta E_t}{kT}\right) \\ C_n N_t \dfrac{n_h n_e}{(n_e + n_h)}; & (n_e + n_h) \gg 2n_i \cdot \cosh\left(\dfrac{\Delta E_t}{kT}\right) \end{cases} \\ R_{ep} = K_{ep} n_{ex} n_h \approx K_{ep}\left(\mu \dfrac{V}{d^2} \dfrac{n_h}{\alpha K_d}\right) \cdot n_h; \quad R_{Lang} \to 0, R_{SRH} \to 0 \end{cases} \tag{7}$$

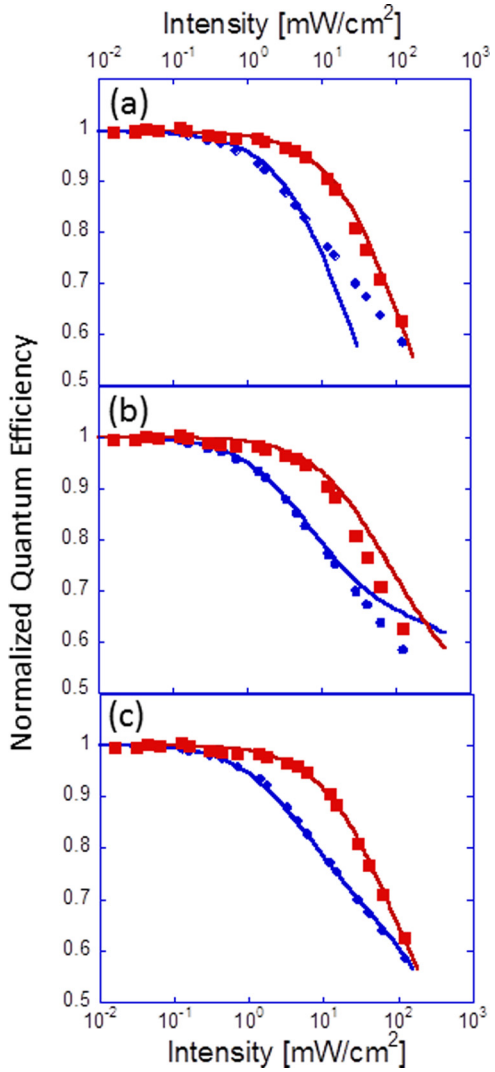

FIG. 4. The normalized quantum efficiency as a function of excitation intensity. Square symbols were measured for the 4 min annealed device and the circles for the 10 min one. The full lines are best fits using Eqs. (3)–(6); (a) assuming the loss mechanisms is only a bimolecular (Langevin charge recombination or exciton annihilation by charge-polaron); (b) assuming the loss mechanism is only trap assisted SRH type; (c) using both bimolecular and SRH type loss mechanisms.

Equation (7) shows that in the absence of other loss mechanism the exciton-polaron loss rate is bimolecular and proportional to n_h^2. This is derived using Eq. (3) which shows that under steady state ($d/dt = 0$) and in the absence of charge recombination ($R_{loss} = 0$) the charge density is linearly proportional to the exciton density. With the above physical framework in mind, in Figure 4 we present the analysis of the quantum efficiency using the trap assisted SRH as well as the bimolecular loss mechanisms. In the analysis we use the parameters in Table I as constants and use the others as fitting parameters.

Figure 4(a) shows best fits assuming only bimolecular loss mechanisms exist with the device. While the device annealed for 4 min can be fitted perfectly with a bimolecular process the 10 min annealing case is definitely not. Moreover, to obtain the fit for the 10 min case, the bimolecular coefficient needs to be enhanced by about a factor of 5. For example, through the fit we obtained $K_{Lang} = 1.5 \times 10^{-12}$ for the 4 min case and $K_{Lang} = 8 \times 10^{-12}$ for the 10 min cases. Turning to the trap assisted Shockley-Read-Hall mechanism we show in Figure 4(b) best fits assuming it is the only loss mechanism. While the fits on the low intensity side seem to be rather good it is clear that the SRH is leveling off at the high intensity regime making it unsuitable as the only loss mechanism. Finally, Figure 4(c) shows best fits using SRH recombination and one of the bimolecular loss mechanisms. The resulting parameters are collected in Table II. By including both SRH and bimolecular terms we find that the bimolecular recombination coefficient does not change between the two annealing times, be it the Langevin (K_{Lang}) or the exciton annihilation (K_{ep}). Regarding the trap assisted recombination we find that the trap density is reduced and that the traps become slightly deeper.

TABLE I. Parameters used as constant in the model.

n_i	$10^8\ cm^{-3}$
C_n	$1.4 \times 10^{-12}\ cm^3\ s^{-1}$ (Ref. 8)
μ	$10^{-4}\ cm^2\ v^{-1}\ s^{-1}$ (Ref. 18)
K_s	$10^{10}\ s^{-1}$ (Ref. 10)

Following the fitting procedures one needs to examine the physical meaning of these fits. First, we find that both trap assisted recombination type of process and bimolecular type one exist within these blends. Regarding the spatial extent of these processes one would expect the electron-hole recombination processes (Langevin or SRH) to take place at the P3HT:PCBM interface and the exciton annihilation at the P3HT phase as it absorbs most of the light. The result showing that the trap density reduces with annealing is consistent with the enhanced phase separation and the resulting lower interface area between the P3HT and PCBM phases. In Ref. 8 we suggested that the traps active in the SRH type recombination are the charge transfer states based on the idea that the recombination takes place across the interface. The deepening of the traps by about 60 meV is in good agreement with reported 50 meV shift of the P3HT HOMO level which was assigned as the cause for the reduction of the energy of charge transfer state.[19]

Turning to the Langevin recombination rate we find, as in Ref. 11, that the only way to justify this process is to detach it from its physical derivation and use K_{Lang} as a fitting parameter that is independent of the charge mobility

TABLE II. Best fit parameters used in Figure 4. In parenthesis are the values that are independent of the parameters indicated in Table I.

	4 min	10 min
N_t [1/cm^3]	2.55×10^{17}	1.28×10^{17}
$(C_n N_t/\mu)$	(2.57×10^9)	(1.79×10^9)
ΔE_t [eV]	0.562	0.493
$\left(2n_i \cdot \cosh\left[\frac{\Delta E_t}{kT}\right]\right)$	(2.44×10^{17})	(1.72×10^{16})
K_{Lang} [cm^3/s]	0.5×10^{-12}	0.5×10^{-12}
K_{ep} [cm^3/s]	2.1×10^{-8}	2.1×10^{-8}
$\left(\frac{K_{ep}}{K_d}\right)$	(2.1×10^{-18})	(2.1×10^{-18})

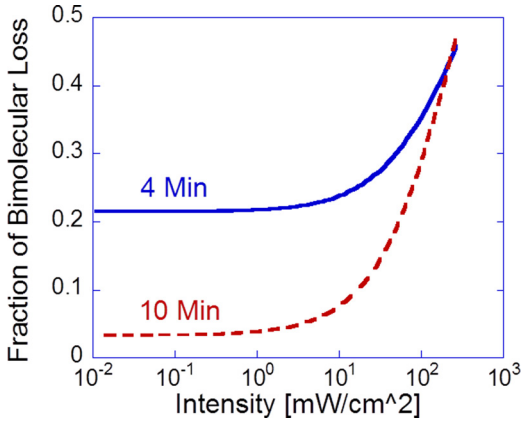

FIG. 5. The deduced fraction of the bimolecular loss as a function of light intensity for the two annealing times.

values. Since the charge recombination can take place only at the P3HT:PCBM interface and we already described such a recombination process using the SRH model, we find the assignment of the bimolecular loss to Langevin recombination inadequate. This is strengthened by the fact that we found the process by which excitons in the P3HT phase are annihilated by hole-polarons to exhibit a signature identical to that of a bimolecular charge recombination process. To the best of our knowledge this process has not been invoked thus far in the context of solar cells. However, PL measurements as a function of light intensity show that this process exists in P3HT:PCBM blends.[10] Also, the value of the coefficient we found (1.6×10^{-8}) is similar to 3×10^{-8} reported in Ref. 10. It is also interesting to note that optimizing charge extraction to reduce bimolecular loss[20] is equally important when the exciton-polaron annihilation is considered instead of the electron-hole Langevin recombination.

To illustrate our point that without probing a wide intensity range it is difficult to extract to underlying physical picture we plot in Figure 5 the relative fraction of the bimolecular loss as deduced using the fitting in Figure 4(c). Figure 5 clearly demonstrates how the dominant process to be probed is dependent on both the processing conditions and the intensity used to probe the physics.

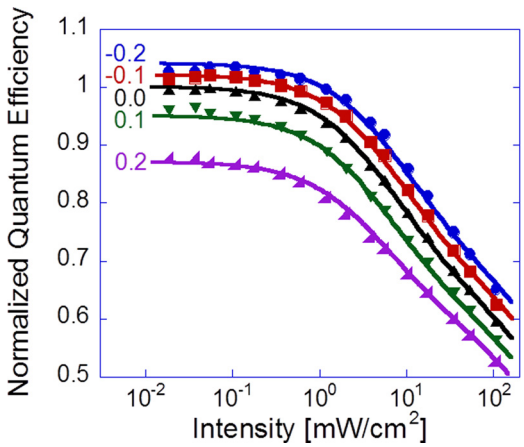

FIG. 6. Measured normalized quantum efficiency (symbols) and fitted efficiency curves (lines) for different applied bias (indicated on the figure). All data were normalized to the efficiency at short circuit bias and $\sim 10^{-2}$ mW/cm^2.

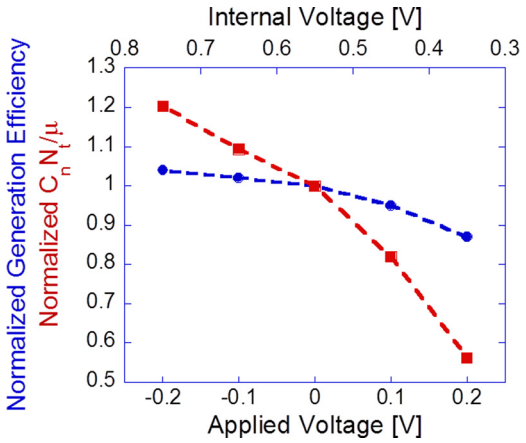

FIG. 7. The bias dependent generation efficiency and of the expression C_nN_t/μ deduced from the fitting in Fig. 6. Curves were normalized to the values found at short circuit conditions. The top X axis shows the internal voltage showing the activated nature of both processes.

Finally, we examine the bias dependence to the efficiency. Figure 6 shows the measured efficiency (symbols) and the respective fitted curves (lines). The applied bias changed between −0.2 V and 0.2 V as depicted on the figure. All values were normalized to the efficiency found for short circuit conditions at the low intensity limit.

Based on the low intensity efficiency it is evident in Figure 6 that the charge generation efficiency (α parameter in Eq. (3)) is bias dependent. The other parameter we needed to change between the curves was the expression C_nN_t/μ which determines the shape of the bias dependent Shockley Read Hall recombination (see Figure 7). The bias dependence of C_nN_t/μ suggests that either the traps recombination (C_nN_t) is activated by the internal voltage or that the mobility (μ) increases as the internal voltage is reduced (note that in the internal voltage range probed diffusion effects are negligible).

To conclude, the charge-polaron induced exciton annihilation is most likely to be the process appearing as a bimolecular loss in bulk hetero-junction organic photovoltaic cells. The relative strength of trap induced recombination and exciton annihilation will determine whether at one sun the efficiency loss appears as monomolecular or bimolecular. We found the trap related recombination loss to be activated, through C_nN_t/μ, by the internal voltage.

This research was partially supported by the Israeli Ministry of Science Tashtiyot program, Israeli Nanotechnology Focal Technology Area project on "Nanophotonics and Detection," the Grand Technion Energy Program (GTEP), and comprises part of The Leona M. and Harry B. Helmsley Charitable Trust reports on Alternative Energy series of the Technion, Israel Institute of Technology, and the Weizmann Institute of Science.

[1]S. Marder, K.-S. Lee, H. Hoppe, and N. Sariciftci, *Photoresponsive Polymers II* (Springer, Berlin/Heidelberg, 2008), Vol. 214, pp. 1–86.
[2]K. M. Coakley and M. D. McGehee, Chem. Mater. **16**(23), 4533–4542 (2004).
[3]B. Kippelen and J. L. Bredas, Energy Environ. Sci. **2**(3), 251–261 (2009).

[4]G. Dennler, M. C. Scharber, and C. J. Brabec, Adv. Mater. **21**(13), 1323–1338 (2009).
[5]J. J. M. Halls, C. A. Walsh, N. C. Greenham, E. A. Marseglia, R. H. Friend, S. C. Moratti, and A. B. Holmes, Nature **376**, 498–500 (1995).
[6]G. Yu, J. Gao, J. C. Hummelen, F. Wudl, and A. J. Heeger, Science **270**(5243), 1789–1791 (1995).
[7]N. Rappaport, O. Solomesch, and N. Tessler, J. Appl. Phys. **98**(3), 033714 (2005).
[8]L. Tzabari and N. Tessler, J. Appl. Phys. **109**(6), 064501 (2011).
[9]M. Pope and C. E. Swenberg, *Electronic Processes in Organic Crystals* (Clarendon Press, Oxford, 1982).
[10]A. J. Ferguson, N. Kopidakis, S. E. Shaheen, and G. Rumbles, J. Phys. Chem. C **112**(26), 9865–9871 (2008).
[11]A. J. Ferguson, N. Kopidakis, S. E. Shaheen, and G. Rumbles, J. Phys. Chem. C **115**(46), 23134–23148 (2011).
[12]I. A. Howard, J. M. Hodgkiss, X. Zhang, K. R. Kirov, H. A. Bronstein, C. K. Williams, R. H. Friend, S. Westenhoff, and N. C. Greenham, J. Am. Chem. Soc. **132**(1), 328–335 (2010).
[13]J. M. Hodgkiss, S. Albert-Seifried, A. Rao, A. J. Barker, A. R. Campbell, R. A. Marsh, and R. H. Friend, Adv. Funct. Mater. **22**(8), 1567–1577 (2012).
[14]J. Nelson, J. Kirkpatrick, and P. Ravirajan, Phys. Rev. B **69**(3), 035337 (2004).
[15]P. W. M. Blom, V. D. Mihailetchi, L. J. A. Koster, and D. E. Markov, Adv. Mater. **19**(12), 1551–1566 (2007).
[16]J. Szmytkowski, J. Phys. D: Appl. Phys. **40**(11), 3352–3357 (2007).
[17]N. Tessler and N. Rappaport, J. Appl. Phys. **96**(2), 1083–1087 (2004).
[18]C. Goh, R. J. Kline, M. D. McGehee, E. N. Kadnikova, and J. M. J. Frechet, Appl. Phys. Lett. **86**(12), 122110 (2005).
[19]T. A. Clarke, M. Ballantyne, J. Nelson, D. D. C. Bradley, and J. R. Durrant, Adv. Funct. Mater. **18**, 4029–4035 (2008).
[20]T. G. J. van der Hofstad, D. Di Nuzzo, S. van Reenen, R. A. J. Janssen, M. Kemerink, and S. C. J. Meskers, J. Phys. Chem. C **117**(7), 3210–3220 (2013).